Sub-single-turnover quantification of enzyme catalysis at ultrahigh throughput via a versatile NAD(P)H coupled assay in microdroplets

Matthew Penner[1,#], Oskar James Klein[1,2,#], Maximillian Gantz[1,#], Sally Boss[2], Paul Barker[2], Paul Dupree[1], Florian Hollfelder[1,]*

[#]*Indicates equal contribution;* [*]*correspondence: fh111@cam.ac.uk*

[1]Department of Biochemistry, University of Cambridge, 80 Tennis Court Rd, Cambridge CB2 1GA, UK
[2]Department of Chemistry, University of Cambridge, Lensfield Road, Cambridge CB2 1EW, UK

Abstract

Enzyme engineering and discovery are crucial for a future sustainable bioeconomy, and harvesting new biocatalysts from large libraries through directed evolution or functional metagenomics requires accessible, rapid assays. Ultra-high throughput screening can often require an optical readout, leading to the use of model substrates that may not accurately report on activity for the target reaction and may require bespoke synthesis. In contrast, coupled assays represent a modular 'plug-and-play' system, where any pairing of enzyme/substrate may be investigated, if the reaction can produce a common intermediate which links the catalytic reaction to a detection cascade readout. Here we establish a detection cascade, producing a fluorescent readout in response to NAD(P)H via glutathione reductase and a subsequent thiol-mediated uncaging reaction, with a 30 nM detection limit. We demonstrate its utility for the glycosidase *AxyAgu*115A (producing monosaccharides from a natural biofuel feedstock) and report a three orders of magnitude improved sensitivity compared to absorbance-based systems, so that less than one catalytic turnover per enzyme molecule expressed from a single cell is detectable. These advantages are brought to bear in plate formats, but also in picoliter emulsion droplets, where enrichments of 950-fold suggest that large libraries can be interrogated against a specific query substrate.

Keywords

Carbohydrate-active enzymes (CAZymes); alpha-glucuronidase; directed protein evolution; droplet microfluidics; biocatalysis; ultrahigh throughput screening assay.

Introduction

Enzyme engineering campaigns rely on functional screening for the discovery of initial hits and subsequent directed evolution[1]. In light of the increasing demand for biocatalysts in the transition towards a sustainable bioeconomy[2], sensitive and high-throughput-compatible assays are crucial for overcoming the challenges arising from target functions that are hard to find in screening libraries to sample the proverbial vastness of sequence space[3,4] in a time-efficient manner[5,6].

Widely used spectroscopic assays rely on model substrates containing aromatic fluorophores or chromophores, released as leaving groups upon enzyme catalysis[4,6–12] but these model substrates rarely emulate the recognition features of many target reactions. Moreover, following directed evolution's basic law "*you get what you screen for*" adaptation of a target enzyme to a model substrate can result in minimal improvements to the desired reaction of a natural substrate[13,14]. Glycosidase discovery and engineering is of great interest for applications including the valorisation of biomass[15], improving medical treatment[16] and as tools for glycobiology[17]. Molecular recognition of the substrate extends far beyond the target glycosidic bond itself, so the specificity towards the local environment within the molecule is critical for glycosidase activity[18], limiting the utility of model substrates that lack some specificity-defining features and creating demand for methods that permit glycosidase screening against natural substrates[19,20].

Coupled assays overcome the challenge of molecular recognition, permitting readout of substrates that are neither fluorogenic nor chromogenic[21,22] by relying on product detection using a cascade centred around a common intermediate, such as NAD(P)H. Thus, with only limited changes in experimental setup, any enzyme coupled to NAD(P)H production or depletion can be assayed. This alleviates the need for tailored synthesis of model substrate probes and thereby provides a versatile platform for assaying $NAD(P)^+$- dependent enzymatic activity. Further, due to the intrinsic specificity of enzymes, such assays are applicable not only in the discovery and engineering of novel enzymes but also as analytical tools for the quantitative detection of small molecules within complex mixtures[23,24]. In such a case, the engineerability of reporter enzymes enables the creation of tailored sensors for a desired analyte.

NAD(P)H-dependant dehydrogenases have important applications in biocatalysis[25,26] (ranging from stereoselective fine chemical synthesis to metabolic engineering) and serve as reporters for the detection of oxidizable groups, which are abundant in many analyte classes[27], for example monosaccharides (resulting from primary enzymatic breakdown of complex carbohydrates). The concurrent reduction of $NAD(P)^+$ to NAD(P)H can be directly monitored by an increase in absorbance at 340 nm. This colorimetric change lies at the heart of many small-molecule quantification kits, such as those sold commercially for monosaccharide detection[28], although the low molar extinction coefficient of NADH limits such assays to a detection limit of 10 μM in plates using direct absorbance of the cofactor[29]. Previous strategies to overcome these limits have focused on coupling NADH reduction to tetrazolium dye reduction[29–31], boosting the measured molar absorption coefficient and improving the signal of the assay 3-fold. However, these dyes are costly and even miniaturized ultrahigh-throughput experiments in microfluidic droplets still suffer from a substantial detection limit of around 10 μM[5,6,29]. This challenge can be overcome using fluorescence

assays, which are often more sensitive than comparable colorimetric assays, as they do not rely on light fully traversing the analyte solution and detect at a wavelength different to the source[32]. While NAD(P)H is itself a fluorophore, its quantum yield is low (2% in aqueous solution leads to no major sensitivity improvement from using fluorescence compared to absorbance in plate format)[33,34], and its fluorescence lifetime and excitation/emission maxima are dependent on protein binding[35,36], complicating assays in complex mixtures, such as cell lysate[37,38]. Coupling a fluorogenic reaction to NAD(P)H production is therefore a compelling alternative, combining the high sensitivity of fluorescent assays with the diversity of available $NAD(P)^+$ small-molecule dehydrogenases, while avoiding the limitations of intrinsic NAD(P)H fluorescence.

In this study, we establish the use of a novel fluorescent dinitrophenyl sulfonyl coumarin probe (thiol-mediated S_NAr Probe, tSNAP) in a coupled assay format for quantification of NAD(P)H-dependent enzymatic activity. We benchmarked the application of tSNAP for the quantification of monosaccharides at ultrahigh-throughput while still matching the detection limit of HPAEC-PAD, cited as the gold-standard column-based method for monosaccharide detection[39–41]. Compared to previously reported coupled assays for NAD(P)H detection in droplets, our system provides a 300-fold improvement in sensitivity and maintains the integrity of the readout over multiple days, enabling extended incubation times. As a proof of concept, we successfully enriched for GH115 glycosidase activity in *E. coli* against the complex substrate beechwood glucuronoxylan, demonstrating the utility of the assay in identifying active biomass-degrading enzymes from a mixture of DNA.

Results and Discussion

1 Sensing nanomolar concentrations of NADH via glutathione-mediated uncaging of tSNAP

To couple NAD(P)H production with turn-on fluorescence, we designed a cascade linking the emergence of NAD(P)H to the formation of free thiols via enzymatic glutathione reduction. The free thiols subsequently uncage a synthesised fluorogenic probe (tSNAP) in a rapid and irreversible S_NAr reaction with a dinitrophenol group that was quenching the coumarin fluorescence[42–45]. Compared to common strategies employing a one-to-one stoichiometry between analyte and reporter, our approach enjoys signal amplification due to the production of two equivalents of reduced glutathione for each equivalent of NAD(P)H consumed. Any NAD(P)H-producing enzyme could be added to this cascade to elicit a fluorogenic response (**Figure 1**). The cascade reagents are cheap and generally accessible – NAD(P)H is re-oxidised by the commercially-available glutathione reductase, so the expensive $NAD(P)^+$ cofactor only needs to be present in catalytic quantities. Synthesis of tSNAP **1** was readily achieved by condensation of 7-hydroxycoumarinyl-4-acetic acid **2** with 2,4-dinitrobenzenesulfonyl chloride in one step from commercially available compounds at 76% yield without the need for purification by chromatography. Initially, the same condensation reaction was attempted using 7-hydroxycoumarinyl-4-acetic acid methyl ester (**I**) and found to be significantly less efficient.

Design of tSNAP was focused around a strongly fluorescent 7-hydroxycoumarin core – as coumarin derivatization is robust and well established, the probe could be readily functionalised[46,47]. To ensure compatibility with microdroplets, leakage into the oil phase or

other droplets had to be prevented. Leakage is a well-documented challenge in microfluidic assay development, preventing the use of the commonly large and aromatic probes for all but the fastest reactions[48–52]. This poses a hitherto unsolved challenge for fluorogenic NAD(P)H quantification as resorufin, the sole published fluorogenic probe for NAD(P)H detection[49,53], is hydrophobic and consequently only compatible with very short reaction times in microfluidic droplets[54]. Previous work has shown that adding charged groups to fluorophores[52] and specifically coumarins[12,55] mitigates droplet leakage and improves aqueous solubility. Therefore, to prevent leakage of tSNAP and its fluorophore product **2**, a carboxylic acid group was incorporated to impart a negative charge on the coumarin scaffold at physiological pH, enabling leakage-free application in droplet microfluidics.

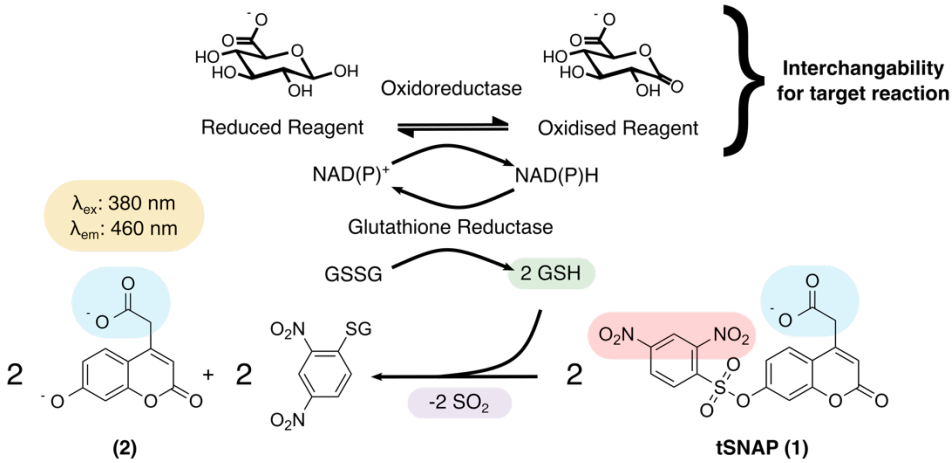

Figure 1: Coupled assay scheme. An analyte (in this case a monosaccharide e.g. produced by a primary glucuronidase reaction, see Fig. 2) is oxidized by a specific dehydrogenase producing NAD(P)H that serves as substrate for glutathione reductase. Reduced glutathione spontaneously reacts with tSNAP **1** forming the coumarin fluorophore product **2** (and the GSH adduct). The design features of tSNAP **1** that make it suitable for NADH detection and droplet screening are highlighted. Around a coumarin core (responsible for fluorescence) electron withdrawing groups on an aromatic ring (red) make tSNAP **1** susceptible to nucleophilic attack by the thiol of GSH (green) and the carboxylate present in tSNAP **1** (blue) causes droplet retention of fluorophore **2**. The release of SO_2 (purple) drives the reaction and the high Stokes Shift (yellow) enables spectroscopic fluorophore quantification.

As the fluorescence of umbelliferone is dependent on its protonation state and therefore the pH of the reaction medium[56], we obtained fluorescence excitation and emission spectra of the 7-hydroxycoumarin fluorophore under different pH conditions (**Figure S1**). Under physiological to slightly basic conditions, the highest signal intensity was achieved with an excitation wavelength of 380 nm coupled to an emission wavelength of 460 nm.

To calibrate the fluorescence signal produced from tSNAP **1**, reduced glutathione (GSH) was added across a concentration range of 25 nM to 25 µM, eliciting a linear response (**Figure 2A**). Formation of the phenylated glutathione product and release of the coumarin fluorophore **2** were confirmed via mass spectroscopy (**Figure S2**). Subsequently, we coupled the S_NAr reaction to the presence of NADH by addition of glutathione reductase. The resulting cascade showed a linear response towards NADH concentration (**Figure 2B**) with a detection limit of 50 nM NADH (corresponding to an amount of 5 pmol NADH) (**Figure S3**) in plates.

2 Detecting picomoles of monosaccharides in high throughput

To demonstrate the sensitivity and modularity of the tSNAP assay, we set out to show its potential for improving small molecule detection limits in high throughput. Monosaccharide quantification is critical for the food industry[24,57], in healthcare applications[58–60] and as a core biochemical technique[61]. Currently, the most sensitive monosaccharide quantification, HPAEC-PAD, requires minutes per single assay, very clean samples[62], and large amounts of costly and sometimes unstable standards[63]. In contrast, high throughput plate-based detection of monosaccharides has sensitivity in the micromolar range at best and can suffer from low selectivity for the monosaccharide of interest[64]. Compared to HPLC-based systems or direct chemical detection, dehydrogenase enzymes are engineerable[65], enabling creation of tailored sensors for any analyte or application. This is the basis of existing kits for NADH-based monosaccharide quantification, but these kits have limits of quantification merely in the low micromolar range[28], and thus a two orders of magnitude sensitivity loss compared to HPAEC-PAD.

Using the coupled assay in plate format and selecting uronate dehydrogenase as a representative coupling enzyme, we were able to linearly detect glucuronic acid with a detection limit of 25 nM (**Figures 2C and S4**). This represents only 5 picomoles of analyte per well, a >100-fold improvement on the best commercially available plate-based glucuronic acid quantification method[28] and more than matches the 12.5 picomole/sample limit of quantification of HPAEC-PAD[61]. In addition to fluorescence end-point measurements, monosaccharides could be also quantified within minutes of reaction initiation using a maximum rate method, enabling shorter analysis times (**Figure S5**). This indicates that this method is a rapid, accessible and derivatisation-free alternative to column-based methods for trace monosaccharide quantification.

To demonstrate the utility of tSNAP for enzyme screening against natural substrates, we set out to test the capacity of the cascade to detect monosaccharide-releasing glycosidases expressed in *E. coli*. In a cellular context, detection cascades risk suffering interference. For example, if background activities in the screening host are too high, excessive background signal can make quantification of target activity impossible. This reduces the capacity of the cascade to detect enzyme activity in cell lysate, thereby limiting its use for high-throughput enzyme screening. Incubating *E. coli* pre-induced for expression of a glucuronoxylan-debranching enzyme (*AxyAgu*115A) with lysis agent, cascade components and glucuronoxylan substrate over an hour-long window revealed that following a brief lag-phase, fluorescence intensity increased far above the negative lysate control, following glucuronic acid release from the polymer (**Figure 2D**). This observation indicates that our coupled assay is suitable for plate-based screening of enzymes even in *E. coli* lysate, the preferred format for plate and droplet-based enzyme engineering and metagenomic screening campaigns.

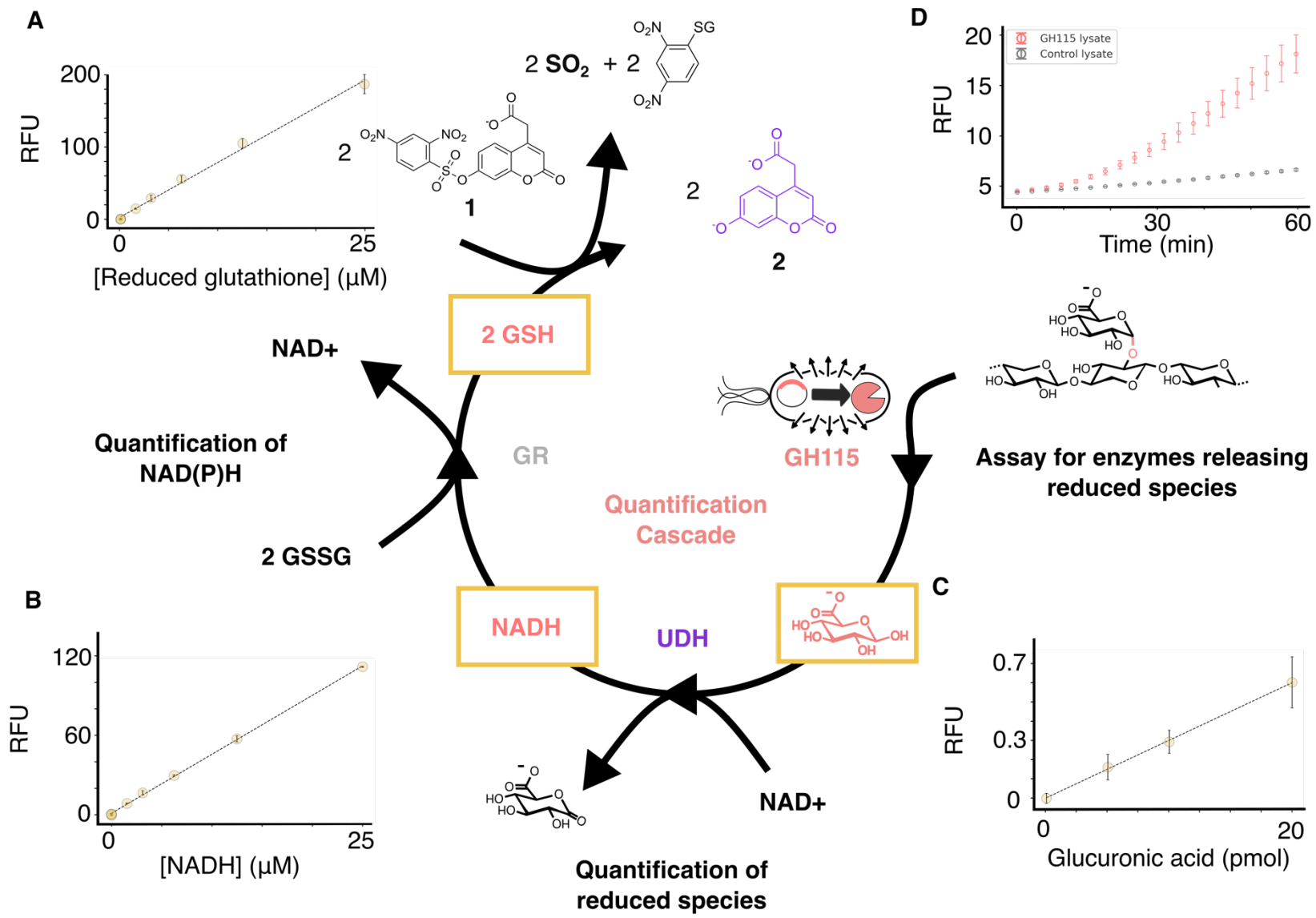
A
RFU
200
100
0
0
25
[Reduced glutathione] (µM)
2 SO2 + 2
O2N
SG
O2N
2
O2N
NO2
1
2
2
D
GH115 lysate
Control lysate
RFU
20
15
10
5
0
30
60
Time (min)
2 GSH
NAD+
Quantification of
NAD(P)H
GR
GH115
Assay for enzymes releasing
reduced species
Quantification
Cascade
2 GSSG
NADH
UDH
C
B
RFU
120
60
0
0
25
[NADH] (µM)
NAD+
Quantification of
reduced species
RFU
0.7
0.3
0
0
20
Glucuronic acid (pmol)

Figure 2: A novel, versatile coupled assay enables detection of trace amounts of monosaccharides in plate format. (A) Unless otherwise stated, all reactions were measured in triplicate at 23 ºC, in 200 mM Tris-HCl (pH 7.0), excited at 380 nm and its emission measured at 460 nm. Quantification of fluorescence emission after reaction completion (after five minutes) shows a linear response to reduced glutathione addition, while the initial rate of reaction was too rapid to be detected using the plate reader. (B) The S_NAr reaction was coupled to glutathione reductase to consume NADH and product quantification was achieved based on a linear calibration curve, in this case using fluorescence emission after thirty minutes of incubation. (C) The cascade can be further coupled to a monosaccharide dehydrogenase (uronate dehydrogenase) facilitating accurate quantification of glucuronic acid concentration with a detection limit of 5 pmol per well, or 25 nM. Superior sensitivity was achieved by using 200 mM Tris-HCl (pH 8.0), and over one hour (the measurement time point) the reaction had reached completion. (D) Time-course of fluorescence emission of GH115-expressing cells with glucuronoxylan substrate and assay components, compared to cells expressing the control enzyme *Sr*IRED, demonstrating that assay can be applied in lysate for quantification of the degradation of complex saccharides or polymers.

3 A novel sensitive coupled assay amenable to ultra-high throughput screening in microfluidic droplets

Much larger numbers of protein variants can be screened in an attractive ultrahigh throughput format where water-in-oil emulsion droplets act as reaction compartments made and handled in microfluidic devices[6]. However, this format has specific limitations that must be overcome, e.g. the transfer of aromatic, hydrophobic fluorescent probes between droplets, likely due to enhanced oil-probe hydrophobic interactions[51]. This leakage results in a loss of signal over time, shortening maximum droplet incubation times and therefore precluding the detection of enzymes that are poorly-expressed or have low activity. Therefore, tSNAP was designed to carry a net negative charge at physiological pH in the form of a carboxylic acid moiety. To demonstrate that the fluorescent coumarin derivative does not leak in microfluidic droplets, we produced two separate populations of droplets, namely those containing the fluorescent product and those without, before mixing the droplets in a collection tube and incubating them for 24h. We imaged the droplets using a fluorescence microscope and no leakage was observed, suggesting compatibility of the assay with the long incubation times often needed to screen for low enzymatic activity in droplets (**Figure 3A**). Further, incubation of a mixed population of droplets containing 25 µM and 50 µM of fluorophore revealed no detectable leakage up to five days. Measuring the same experiment again at day 16 showed that the fluorescence of the two populations had begun to converge (by 73% of their original fluorescence). However, the individual populations could still be distinguished (**Figure 3A**) with only 3% overlap. This stands in contrast to the NAD(P)H probe resorufin – fluorescence microscopy revealed near complete equilibration of previously empty and full droplets in only 6 hours[54], suggesting at least a 64-fold better retention of the uncaged fluorophore.

However, leakage of product was not the only consideration, as all active components of a successful cascade should be retained within each droplet to prevent cross-talk. Therefore, we mixed a population of droplets containing either cascade reagents with or without monosaccharide. Signal appeared rapidly on-chip, and the integrity of the populations remained intact after extended incubation periods (**Figure 3B**). These results demonstrate that the entire cascade is compatible with FADS, allowing for sensitive and rapid assaying even after long incubation times[66].

Sensitivity is a major limitation of several droplet-based detection modes as for example absorbance-based detection (~10 µM)[29,67], which currently is the only method available for screening dehydrogenase activity using non-model substrates at ultrahigh throughput that does not suffer from leakage[54,68]. Fluorescent assays can be up to three orders of magnitude more sensitive, as shown by Colin *et al* for a fluorescein-based phosphotriesterase assay with a detection limit of 2.5 nM[4]. This sensitivity allows detection of enzymatic activities that lead to less than one turnover per enzyme molecule, suitable even when expression or intrinsic activity are low. We benchmarked the theoretical detection limit with the coumarin product **2** in droplets and showed linear dependence of fluorescence and product concentration down to 30 nM (corresponding to 542,000 molecules per droplet, or 271,000 turnovers of glutathione reductase), with the lowest quantified droplet populations (30 nM and 44 nM) yielding populations that can be clearly distinguished (**Figures 3C and S6**).

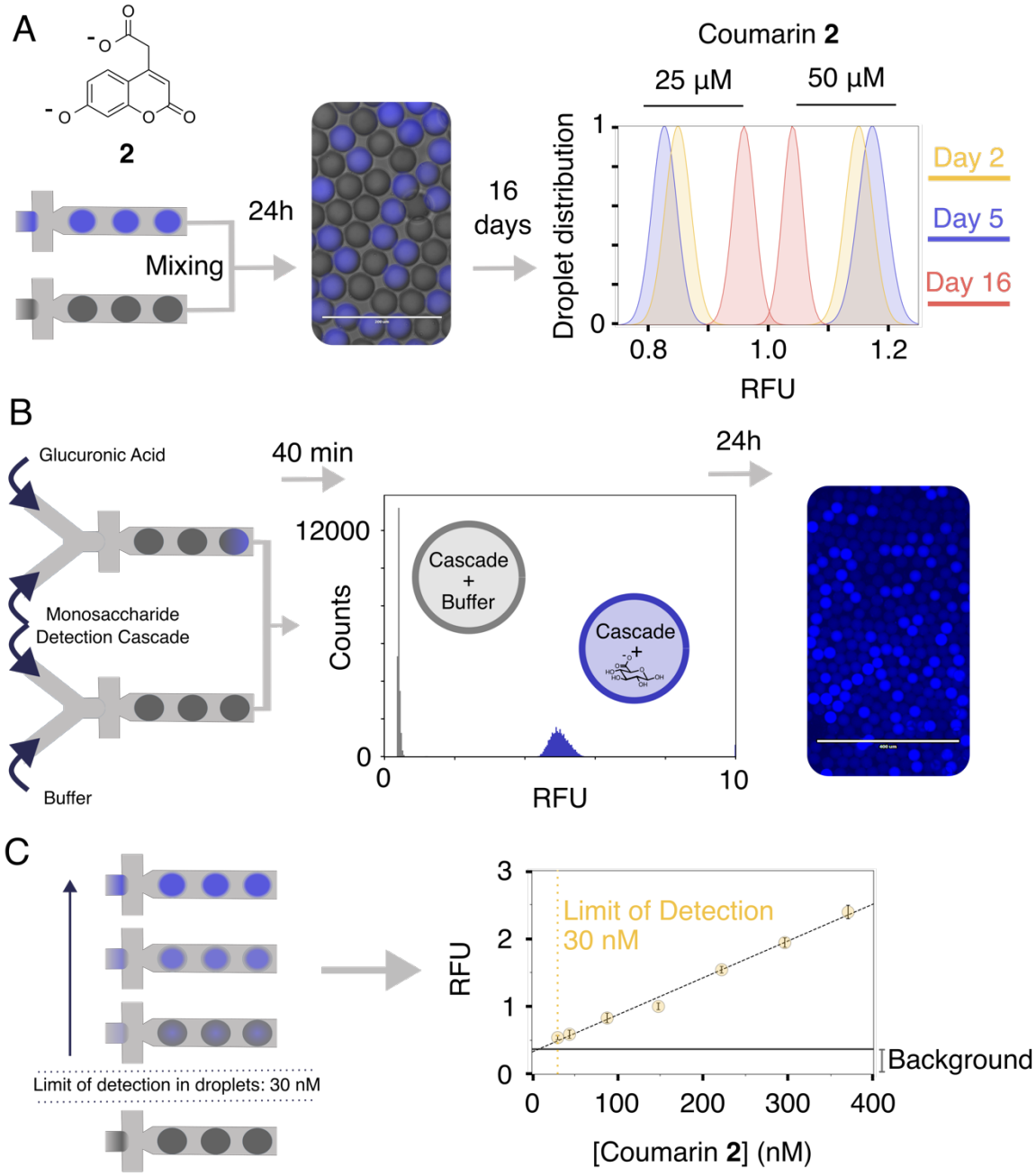

Figure 3: Droplet application of the coupled assay yields a sensitive and stable signal that emerges rapidly. (A) Droplets with 150 µM coumarin product incubated overnight with droplets containing no product shows no detectable transfer of fluorescent compound between droplets (measured at 358 nm). Further, co-incubation of droplets containing 25 µM or 50 µM fluorescent compound for up to 16 days maintained two distinct fluorescent populations when measured on-chip. (B) Droplets with cascade reagents and 500 µM glucuronic acid or cascade reagents and buffer form two distinct populations on a FADS sorter when mixed, incubated for 40 min, and measured together. Fluorescence microscopy of the same mixed population incubated overnight, measured at 358 nm reveals no visible leakage, indicating that the cascade components are suitable for extended incubation. (C) Droplet populations with seven concentrations of pure coumarin product measured at 375 nm in a FADS setup reveal the 30 nM detection limit of fluorophore on-chip. Values are averages of ~10,000 size-gated droplets and error bars represent the standard deviation within this population.

4 Droplet-based enrichment demonstrates ultrahigh-throughput compatibility of the tSNAP assay and enables fluorescence-based glycosidase screening against natural substrates

Ultrahigh throughput application of this coupled assay for reactions yielding oxidizable species (such as monosaccharides) has been achieved here in a two-step microfluidic workflow as outlined in **Figure 4A.** Following expression of a cytoplasmic enzyme library in bulk media, cells are co-encapsulated with target substrate, coupled assay and lysis reagents. The droplets are then subjected to an incubation over a suitable timeframe to reach the limit of detection (at least 271,000 enzyme turnovers), and the droplets are then sorted using fluorescence-activated cell sorting (FADS). By selecting the droplets with the strongest fluorescence emission, the sorted library is enriched in the most active members.
The modular approach presented here enables ultra-high throughput screening for previously inaccessible enzymatic activity without the requirement for synthetically challenging model substrates. We demonstrate this by enriching a glycosidase enzyme from a mock library containing a 1000-fold abundance of inactive mutants (**Figures S7 and S8**). We selected the GH115 family of glucuronoxylan debranching enzymes, which liberate the monosaccharide glucuronic acid from the heterogenous polysaccharide (**Figure 4B**) and have previously been inaccessible to ultra-high throughput screening partly due to its intolerance for model substrates. The model substrate pNP-glucuronide shows a 36,000-fold lower k_{cat} when compared to activity against polymeric xylan, requiring extremely long incubation times to detect activity[66].

The mock library was encapsulated and droplets were stored off-chip for 60 minutes, after which the most fluorescent 0.02% of droplets were sorted at 800 Hz using FADS **(Figure 4C)**. DNA from the sorted population was recovered by transformation into *E. coli*. Single clones were analysed using a functional assay for glucuronic acid release from beechwood xylan based on NADH absorbance, revealing 43% positive variants in the sorted population (**Figures 4C and S9**) and thus an enrichment of 950-fold, according to the method of Baret et al[69] (**Supplementary Note 1**). We have therefore demonstrated effective application of this assay cascade at ultra-high throughput, highlighting its potential uses in functional metagenomics or directed evolution campaigns, which will be more likely to succeed with these exquisitely low limits of detection.

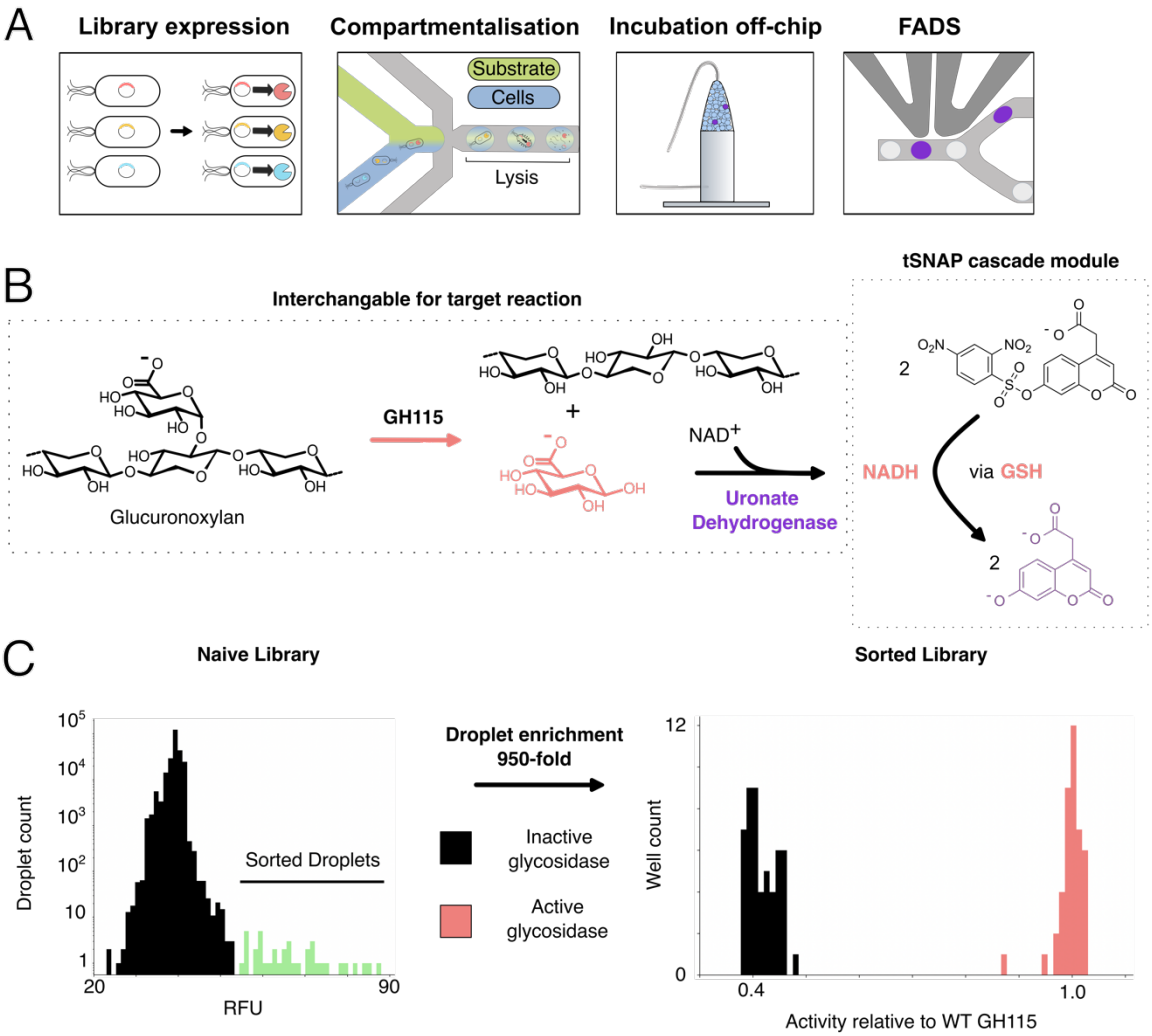

Figure 4: A novel sensitive droplet assay detects glycosidase activity from single cells on natural substrates.
(A) Workflow used for testing the enrichment of glycosidases in droplets. (B) Schematic of the target droplet reaction in this assay. (C) (*Left*) Width-gated histogram describing a sample of droplet RFUs in the unsorted library. The top 0.02% of droplets were selected for sorting. (Right) Plate activity of sorted clones picked from the recovered library relative to the wild type. 39 of the 90 clones assayed were found to be confidently positive.

Conclusion

Our novel, ultra-high throughput fluorogenic NAD(P)H assay achieves single turnover sensitivity in the context of a coupled enzyme assay that can potentially be generalised to a wide range of biocatalytic processes that involve this cofactor. Demonstrated here for the xylan α-glucuronidase AxyAgu115A, dehydrogenase-coupled assays have been established for many other glycosidases such as xylosidases, glucosidases and arabinosidases[68], and can be implemented for other functions based on the modularity principle of our assay, where the coupled specific redox enzyme is exchanged (depending on the product of the primary reaction) and the generalised downstream detection machinery remains in place. Primary reactions that can similarly be coupled to NAD(P)H production include e.g. small-molecule/natural product methyltransferases[70], nucleotide methyltransferases[71], ATPases and other enzymes that produce ADP[72], and systems that produce urea[73] or pyruvate, amino acid oxidative deaminases[74] and phosphite dehydrogenases[75]. Finally, engineering of redox

enzymes that are not in a coupled set-up, such dehydrogenases for biocatalytic applications[76,77], including conversion of monosaccharides to hydrogen gas[78], will directly benefit from a sensitive screening assay. Indeed, detection of low-activity enzymes is crucial for protein engineering and discovery of biocatalysts[79–81], because the recruitment of proteins for the conversion of our current economic model to a sustainable bioeconomy depends on three sources with typically weak activities: (i) promiscuous side activities of existing enzymes[82,83], (ii) enzymes from metagenomic sources[84], identified by functional screening or by bioinformatics and (iii) computationally designed enzymes[79–81]. Without a sensitive assay, these useful, but imperfect starting points cannot be improved by directed evolution and compatibility with an ultrahigh throughput method is crucial for success. Droplet microfluidics is arguably one of the most powerful UHT formats, allowing screening of ~10^7-membered libraries in a day. Using this technology, aqueous-to-oil phase transfer of the product analyte can thwart early evolution campaigns when extended droplet incubation is necessary to bring about sufficient turnover to be detectable. In addition to the improved sensitivity of our assay, the presence of a charged moiety (at physiological pH) on the fluorophore alleviates leakage, making such long-term experiments possible. In keeping with Arnold's first law of directed evolution ('*you get what you screen for*'[13]), it is remarkable that here *natural* glycosidase substrates can be used (instead of widely used fluorogenic model substrates with different molecular recognition properties and reactivities[85]). Limited catalytic improvements towards natural target substrates are often found when activity towards substrates with fluorogenic or chromogenic leaving groups is used as the selection criterion[85] e.g. fluorescein[85] or pNP [86] conjugates, or by other changes in the substrate structure, such as azide substitutions[87]. Indeed, GH115-family enzymes react more than four orders of magnitude slower for such substrates (e.g. pNP-glucuronide) than their polymeric xylan targets[66]. We demonstrate the utility of this assay with an enrichment of GH115 xylan α-glucuronidase from a population of low activity variants using UHT droplet screening, based on activity against a polymeric xylan substrate deriving from beechwood. This example paves the way for ultrahigh throughput screening of biocatalysts with a role in biofuel production[88] as an example for the conversion of biomass waste streams into high-value chemicals[89] and makes the case that this assay is ready for deployment in directed evolution or functional metagenomic campaigns that are currently not feasible.

Acknowledgements

The authors thank Prof. Emma Master for a gene string for *AxyAgu*115A, Dr Tomasz Kaminski for microfluidic chip fabrication and members of the Hollfelder lab for helpful discussions and comments. This work was supported by the European Union's Horizon 2020 research and innovation programme via an ERC Advanced Investigator grant (to FH; 695669), by the Biological and Biotechnological Research Council (BB/W006391/1) and the Volkswagen Foundation (98182). O.J.K. was supported by an EPSRC studentship (EP/R513180/1). S.B. and P.B. thank the Chemistry Department at Cambridge University for financial support.

References

[1] F. H. Arnold, *Angew Chem Int Ed* **2019**, *58*, 14420–14426.
[2] E. Radley, J. Davidson, J. Foster, R. Obexer, E. L. Bell, A. P. Green, *Angew. Chem. Int. Ed.* **n.d.**, *n/a*, e202309305.
[3] P. Lorenz, J. Eck, *Nat. Rev. Microbiol.* **2005**, *3*, 510–516.

[4] P.-Y. Colin, B. Kintses, F. Gielen, C. M. Miton, G. Fischer, M. F. Mohamed, M. Hyvönen, D. P. Morgavi, D. B. Janssen, F. Hollfelder, *Nat. Commun.* **2015**, *6*, 10008.
[5] M. Gantz, G. A. Aleku, F. Hollfelder, *Trends Biochem. Sci.* **2022**, *47*, 451–452.
[6] M. Gantz, S. Neun, E. J. Medcalf, L. D. van Vliet, F. Hollfelder, *Chem. Rev.* **2023**, *123*, 5571–5611.
[7] S. Neun, P. Brear, E. Campbell, T. Tryfona, K. El Omari, A. Wagner, P. Dupree, M. Hyvönen, F. Hollfelder, *Nat. Chem. Biol.* **2022**, *18*, 1096–1103.
[8] J. D. Schnettler, O. J. Klein, T. S. Kaminski, P.-Y. Colin, F. Hollfelder, *J. Am. Chem. Soc.* **2023**, *145*, 1083–1096.
[9] J. D. Schnettler, M. S. Wang, M. Gantz, C. Karas, F. Hollfelder, M. H. Hecht, **2023**, 2023.02.13.528392.
[10] R. Obexer, A. Godina, X. Garrabou, P. R. E. Mittl, D. Baker, A. D. Griffiths, D. Hilvert, *Nat. Chem.* **2017**, *9*, 50–56.
[11] F. Ma, M. T. Chung, Y. Yao, R. Nidetz, L. M. Lee, A. P. Liu, Y. Feng, K. Kurabayashi, G.-Y. Yang, *Nat. Commun.* **2018**, *9*, 1030.
[12] H.-M. Chen, S. A. Nasseri, P. Rahfeld, J. F. Wardman, M. Kohsiek, S. G. Withers, *Org. Biomol. Chem.* **2021**, *19*, 789–793.
[13] L. You, F. H. Arnold, *Protein Eng.* **1996**, *9*, 77–83.
[14] M. Wang, T. Si, H. Zhao, *Bioresour. Technol.* **2012**, *115C*, 117–125.
[15] U. Bornscheuer, K. Buchholz, J. Seibel, *Angew. Chem. Int. Ed.* **2014**, *53*, 10876–10893.
[16] P. Rahfeld, L. Sim, H. Moon, I. Constantinescu, C. Morgan-Lang, S. J. Hallam, J. N. Kizhakkedathu, S. G. Withers, *Nat. Microbiol.* **2019**, *4*, 1475–1485.
[17] F. Goubet, P. Jackson, M. J. Deery, P. Dupree, *Anal. Biochem.* **2002**, *300*, 53–68.
[18] V. N. Perna, K. Barrett, A. S. Meyer, B. Zeuner, *Glycobiology* **2023**, *33*, 396–410.
[19] V. R. Pidatala, A. Mahboubi, J. C. Mortimer, *J. Vis. Exp. JoVE* **2017**, 56424.
[20] C. A. Santos, M. A. B. Morais, O. M. Terrett, J. J. Lyczakowski, L. M. Zanphorlin, J. A. Ferreira-Filho, C. C. C. Tonoli, M. T. Murakami, P. Dupree, A. P. Souza, *Sci. Rep.* **2019**, *9*, 4903.
[21] S. Hecko, A. Schiefer, C. P. S. Badenhorst, M. J. Fink, M. D. Mihovilovic, U. T. Bornscheuer, F. Rudroff, *Chem. Rev.* **2023**, *123*, 2832–2901.
[22] M. J. Menke, P. Pascal Schneider, C. P. S. Badenhorst, A. Kunzendorf, F. Heinz, M. Dörr, M. A. Hayes, U. Bornscheuer, *Angew. Chem. Int. Ed.* **n.d.**, *n/a*, e202313912.
[23] J. A. Bauer, M. Zámocká, J. Majtán, V. Bauerová-Hlinková, *Biomolecules* **2022**, *12*, 472.
[24] C. Garcia-Hernandez, C. Garcia-Cabezon, F. Martin-Pedrosa, M. L. Rodriguez-Mendez, *Food Chem.* **2019**, *289*, 751–756.
[25] K. Bachosz, J. Zdarta, L. D. Nghiem, T. Jesionowski, *Environ. Technol. Innov.* **2022**, *28*, 102874.
[26] C. J. Hartley, C. C. Williams, J. A. Scoble, Q. I. Churches, A. North, N. G. French, T. Nebl, G. Coia, A. C. Warden, G. Simpson, A. R. Frazer, C. N. Jensen, N. J. Turner, C. Scott, *Nat. Catal.* **2019**, *2*, 1006–1015.
[27] L. Sellés Vidal, C. L. Kelly, P. M. Mordaka, J. T. Heap, *Biochim. Biophys. Acta BBA - Proteins Proteomics* **2018**, *1866*, 327–347.
[28] Megazyme, "D-glucuronic acid & d-galacturonic acid (d-glucuronate & d-galacturonate) assay procedure," can be found under https://www.megazyme.com/documents/Assay_Protocol/K-URONIC_DATA.pdf, **2019**.
[29] F. Gielen, R. Hours, S. Emond, M. Fischlechner, U. Schell, F. Hollfelder, *Proc. Natl. Acad. Sci. U. S. A.* **2016**, *113*, E7383–E7389.
[30] J. R. Marshall, P. Yao, S. L. Montgomery, J. D. Finnigan, T. W. Thorpe, R. B. Palmer, J. Mangas-Sanchez, R. A. M. Duncan, R. S. Heath, K. M. Graham, D. J. Cook, S. J. Charnock, N. J. Turner, *Nat. Chem.* **2021**, *13*, 140–148.
[31] P. J. Zurek, P. Knyphausen, K. Neufeld, A. Pushpanath, F. Hollfelder, *Nat. Commun.* **2020**, *11*, 6023.
[32] J. R. Lakowicz, Ed. , *Principles of Fluorescence Spectroscopy*, Springer US, Boston, MA, **2006**.

[33] I. A. Gorbunova, M. K. Danilova, M. E. Sasin, V. P. Belik, D. P. Golyshev, O. S. Vasyutinskii, *J. Photochem. Photobiol. Chem.* **2023**, *436*, 114388.
[34] A. Swoboda, L. J. Pfeifenberger, Z. Duhović, M. Bürgler, I. Oroz-Guinea, K. Bangert, F. Weißensteiner, L. Parigger, K. Ebner, A. Glieder, W. Kroutil, *Angew. Chem. Int. Ed Engl.* **2023**, *62*, e202312721.
[35] S. F. Velick, *J. Biol. Chem.* **1958**, *233*, 1455–1467.
[36] J. C. Brochon, P. Wahl, M. O. Monneuse-Doublet, A. Olomucki, *Biochemistry* **1977**, *16*, 4594–4599.
[37] T. M. Cannon, J. L. Lagarto, B. T. Dyer, E. Garcia, D. J. Kelly, N. S. Peters, A. R. Lyon, P. M. W. French, C. Dunsby, *Osa Contin.* **2021**, *4*, 1610–1625.
[38] N. Ma, M. A. Digman, L. Malacrida, E. Gratton, *Biomed. Opt. Express* **2016**, *7*, 2441–2452.
[39] J. C. Mortimer, G. P. Miles, D. M. Brown, Z. Zhang, M. P. Segura, T. Weimar, X. Yu, K. A. Seffen, E. Stephens, S. R. Turner, P. Dupree, *Proc. Natl. Acad. Sci.* **2010**, *107*, 17409–17414.
[40] F. Goubet, C. J. Barton, J. C. Mortimer, X. Yu, Z. Zhang, G. P. Miles, J. Richens, A. H. Liepman, K. Seffen, P. Dupree, *Plant J.* **2009**, *60*, 527–538.
[41] H. Temple, P. Phyo, W. Yang, J. J. Lyczakowski, A. Echevarría-Poza, I. Yakunin, J. P. Parra-Rojas, O. M. Terrett, S. Saez-Aguayo, R. Dupree, A. Orellana, M. Hong, P. Dupree, *Nat. Plants* **2022**, *8*, 656–669.
[42] B. Zhang, C. Ge, J. Yao, Y. Liu, H. Xie, J. Fang, *J. Am. Chem. Soc.* **2015**, *137*, 757–769.
[43] A. Shao, Q. Xu, C. W. Kang, C. F. Cain, A. C. Lee, C.-H. A. Tang, J. R. Del Valle, C.-C. A. Hu, *Mol. Pharm.* **2022**, *19*, 1059–1067.
[44] H. Maeda, H. Matsuno, M. Ushida, K. Katayama, K. Saeki, N. Itoh, *Angew. Chem. Int. Ed.* **2005**, *44*, 2922–2925.
[45] B. Roubinet, P.-Y. Renard, A. Romieu, *Dyes Pigments* **2014**, *110*, 270–284.
[46] S. M. Basavarajaiah, N. Gunavanthrao Yernale, M. Punith Kumar, B. Rakesh, *Polycycl. Aromat. Compd.* **2023**, *0*, 1–25.
[47] A. Bouhaoui, M. Eddahmi, M. Dib, M. Khouili, A. Aires, M. Catto, L. Bouissane, *ChemistrySelect* **2021**, *6*, 5848–5870.
[48] A. Zinchenko, S. R. A. Devenish, F. Hollfelder, **2023**, 2023.04.23.538007.
[49] A. Debon, M. Pott, R. Obexer, A. P. Green, L. Friedrich, A. D. Griffiths, D. Hilvert, *Nat. Catal.* **2019**, *2*, 740–747.
[50] A. P. Debon, R. C. R. Wootton, K. S. Elvira, *Biomicrofluidics* **2015**, *9*, 024119.
[51] E. M. Payne, M. Taraji, B. E. Murray, D. A. Holland-Moritz, J. C. Moore, P. R. Haddad, R. T. Kennedy, *Anal. Chem.* **2023**, *95*, 4662–4670.
[52] F. Courtois, L. F. Olguin, G. Whyte, A. B. Theberge, W. T. S. Huck, F. Hollfelder, C. Abell, *Anal. Chem.* **2009**, *81*, 3008–3016.
[53] M. Gimeno-Pérez, J. D. Finnigan, C. Echeverria, S. J. Charnock, A. Hidalgo, D. M. Mate, *ChemSusChem* **2022**, *15*, e202102750.
[54] M. Klaus, P. J. Zurek, T. S. Kaminski, A. Pushpanath, K. Neufeld, F. Hollfelder, *ChemBioChem* **2021**, *22*, 3292–3299.
[55] G. Woronoff, A. El Harrak, E. Mayot, O. Schicke, O. J. Miller, P. Soumillion, A. D. Griffiths, M. Ryckelynck, *Anal. Chem.* **2011**, *83*, 2852–2857.
[56] D. W. Fink, W. R. Koehler, *Anal. Chem.* **1970**, *42*, 990–993.
[57] G. Jayanthi Kalaivani, S. K. Suja, *Food Chem.* **2019**, *298*, 124981.
[58] Y. Chen, Q. Yao, X. Zeng, C. Hao, X. Li, L. Zhang, P. Zeng, *Front. Oncol.* **2022**, *12*, 1014159.
[59] B. Han, J. W. Park, M. Kang, B. Kim, J. Jeong, O.-S. Kwon, J. Son, *J. Chromatogr. B* **2020**, *1160*, 122370.
[60] P. Mohammadnejad, S. S. Asl, S. Aminzadeh, K. Haghbeen, *Spectrochim. Acta. A. Mol. Biomol. Spectrosc.* **2020**, *229*, 117897.
[61] Z. Zhang, N. M. Khan, K. M. Nunez, E. K. Chess, C. M. Szabo, *Anal. Chem.* **2012**, *84*, 4104–4110.
[62] T. R. I. Cataldi, D. Nardiello, *J. Agric. Food Chem.* **2003**, *51*, 3737–3742.

[63] M. Kurzyna-Szklarek, J. Cybulska, A. Zdunek, *Food Chem.* **2022**, *394*, 133466.
[64] N. N. Deshavath, G. Mukherjee, V. V. Goud, V. D. Veeranki, C. V. Sastri, *Int. J. Biol. Macromol.* **2020**, *156*, 180–185.
[65] A. F. Geiss, T. M. B. Reichhart, B. Pejker, E. Plattner, P. L. Herzog, C. Schulz, R. Ludwig, A. K. G. Felice, D. Haltrich, *ACS Sustain. Chem. Eng.* **2021**, *9*, 7086–7100.
[66] W. Wang, R. Yan, B. P. Nocek, T. V. Vuong, R. D. Leo, X. Xu, H. Cui, P. Gatenholm, G. Toriz, M. Tenkanen, A. Savchenko, E. R. Master, *J. Biol. Chem.* **2016**, *291*, 14120–14133.
[67] E. J. Medcalf, M. Gantz, T. S. Kaminski, F. Hollfelder, *Anal. Chem.* **2023**, *95*, 4597–4604.
[68] S. Ladeveze, P. J. Zurek, T. S. Kaminski, S. Emond, F. Hollfelder, *ACS Catal.* **2023**, *13*, 10232–10243.
[69] J.-C. Baret, O. J. Miller, V. Taly, M. Ryckelynck, A. El-Harrak, L. Frenz, C. Rick, M. L. Samuels, J. B. Hutchison, J. J. Agresti, D. R. Link, D. A. Weitz, A. D. Griffiths, *Lab. Chip* **2009**, *9*, 1850–1858.
[70] H. Simon-Baram, S. Roth, C. Niedermayer, P. Huber, M. Speck, J. Diener, M. Richter, S. Bershtein, *ChemBioChem* **2022**, *23*, e202200162.
[71] B. P. S. Chouhan, S. Maimaiti, M. Gade, P. Laurino, *Biochemistry* **2019**, *58*, 166–170.
[72] L. Radnai, R. F. Stremel, J. R. Sellers, G. Rumbaugh, C. A. Miller, *J. Vis. Exp. JoVE* **2019**, 10.3791/60017.
[73] H. Kaltwasser, H. G. Schlegel, *Anal. Biochem.* **1966**, *16*, 132–138.
[74] H. Q. Smith, C. Li, C. A. Stanley, T. J. Smith, *Neurochem. Res.* **2019**, *44*, 117–132.
[75] H. A. Relyea, W. A. van der Donk, *Bioorganic Chem.* **2005**, *33*, 171–189.
[76] A. S. de Miranda, C. D. F. Milagre, F. Hollmann, *Front. Catal.* **2022**, *2*.
[77] W. Kroutil, H. Mang, K. Edegger, K. Faber, *Curr. Opin. Chem. Biol.* **2004**, *8*, 120–126.
[78] J. Woodward, S. M. Mattingly, M. Danson, D. Hough, N. Ward, M. Adams, *Nat. Biotechnol.* **1996**, *14*, 872–874.
[79] O. Khersonsky, D. Röthlisberger, A. M. Wollacott, P. Murphy, O. Dym, S. Albeck, G. Kiss, K. N. Houk, D. Baker, D. S. Tawfik, *J. Mol. Biol.* **2011**, *407*, 391–412.
[80] O. Khersonsky, D. Röthlisberger, O. Dym, S. Albeck, C. J. Jackson, D. Baker, D. S. Tawfik, *J. Mol. Biol.* **2010**, *396*, 1025–1042.
[81] D. Röthlisberger, O. Khersonsky, A. M. Wollacott, L. Jiang, J. DeChancie, J. Betker, J. L. Gallaher, E. A. Althoff, A. Zanghellini, O. Dym, S. Albeck, K. N. Houk, D. S. Tawfik, D. Baker, *Nature* **2008**, *453*, 190–195.
[82] R. A. Jensen, *Annu. Rev. Microbiol.* **1976**, *30*, 409–425.
[83] P. J. O'Brien, D. Herschlag, *Chem. Biol.* **1999**, *6*, R91–R105.
[84] P. D. Schloss, J. Handelsman, *Curr. Opin. Biotechnol.* **2003**, *14*, 303–310.
[85] E. Hardiman, M. Gibbs, R. Reeves, P. Bergquist, *Appl. Biochem. Biotechnol.* **2010**, *161*, 301–312.
[86] K. Mewis, N. Lenfant, V. Lombard, B. Henrissat, *Appl. Environ. Microbiol.* **2016**, *82*, 1686–1692.
[87] F. Liu, H.-M. Chen, Z. Armstrong, S. G. Withers, *ACS Cent. Sci.* **2022**, *8*, 656–662.
[88] L. S. McKee, H. Sunner, G. E. Anasontzis, G. Toriz, P. Gatenholm, V. Bulone, F. Vilaplana, L. Olsson, *Biotechnol. Biofuels* **2016**, *9*, 2.
[89] T. V. Vuong, E. R. Master, *Biotechnol. Biofuels* **2020**, *13*, 51.